

# Human Drivers Based Active-Passive Model for Automated Lane Change

Quoc Huy Do and Seiichi Mita  
*The Research Center for Smart Vehicles,  
Toyota Technological Institute,  
Nagoya, Japan  
E-mail: huydq@toyota-ti.ac.jp,  
smita@toyota-ti.ac.jp)*

Hossein Tehrani, Masumi Egawa,  
and Kenji Muto  
*Corporate R&D Div.3, DENSO CORPORATION,  
Kariya, Aichi, Japan  
E-mail: hossein.tehrani@denso.co.jp,  
masumi\_egawa@denso.co.jp,  
kenji\_muto@denso.co.jp*

Keisuke Yoneda  
*Previously, the Research Center for Smart Vehicles, Toyota Technological Institute, Nagoya, Japan. Currently, Autonomous Vehicle Research Unit, Institute for Frontier Science Initiative, Kanazawa University.  
E-mail: k.yoneda@staff.kanazawa-u.ac.jp*

Digital Object Identifier 10.1109/MITS.2016.2613913  
Date of publication: 19 January 2017



©STOCKPHOTO.COM/SINOPICS

**Abstract**—Lane change maneuver is a complicated maneuver, and incorrect maneuvering is an important reason for expressway accidents and fatalities. In this scenario, automated lane change has great potential to reduce the number of accidents. Previous research in this area, typically, focuses on the generation of an optimal lane change trajectory, while ignoring the human behavior model. To understand the human lane change behavior model, we carried out experiments on Japanese expressways. By analyzing the human-driver lane change data, we propose a two-segment lane change model that mimics the human-driver. We categorize the driving environment based on the observation grid and propose different lane change behaviors to handle the different scenarios. We develop an intuitive

method to select the suitable lane change behavior, for a given scenario, using active (accelerate/decelerate) and passive (wait) information derived from the distance and related velocity ( $dx/dv$ ) graph. Additionally, we also identify the most desirable and safe conditions for doing lane change based on the human driver preference data. We evaluated the proposed model by performing lane change simulations in the PreScan environment, while considering the vehicle motion/control model. The simulation results show the proposed model is able to handle complicated lane change scenarios with human driver-like performance.

## I. Introduction

**S**tatistical data of expressway traffic accidents shows that human error is a major reason for nearly 90% of accidents (Volvo 2013) [1]. Lane change maneuver is a cause for many serious expressway accidents due to the wrong estimation of surrounding environment or wrong maneuvering. Currently, ADAS or automated driving has demonstrated the potential to reduce the impact of human errors.

The literature in lane change or overtaking maneuver-based ADAS can be divided into rule-based [2], [3] or utility-based [4] approaches. In [5] and [6], Kasper et al. introduced an object-oriented Bayesian network approach to model the traffic scene for the detection of lane change maneuvers. Bayesian network was also used by Schubert et al. [7] for lane change situation assessment and decision making. In [8], the authors model the surrounding environment into an occupancy grid, and then apply dynamic programming to find drivable cells, before utilizing decision making to either maintain the lane or perform lane change. Other related researches focus on maneuver prediction. In [9], [10] authors trained a neural network for the prediction of the future lane change trajectory. A dynamic Bayesian network is also used by Gindelé et al. [11] and Schlechtriemen et al. [12], [13] for the behavior and trajectory prediction. Meanwhile, Kumar et al. [14] utilized the support vector machine and Bayesian filter for the same purpose. The fuzzy logic was used by Naranjo et al. [15] for modelling the lane change decision making. They use fuzzy controllers that mimic human behavior and reactions during overtaking maneuvers. Bahram et al. [16] proposed a decision making based on a nonlinear model predictive approach. Mixed logical dynamical system is also used for solving lane change decision making as in [17]–[19]. Simon and Markus [20] applied an online Partially Observable Markov Decision Process to solve the decision making for lane change. Brechtel et al. [21] applied probabilistic MDP-Behavior planning for cars. Ardel et al. [22] presented a probabilistic approach to build a lane change framework for automated vehicles. A lane selection method was proposed by Jin et al. [23], however, this method requires all related

vehicles to be connected. In [24], authors presented a collision avoidance method by analyzing the kinematic model of the vehicle and then calculated the minimum safety space requirement for performing the lane change. Other methods for lane change based on safety space checking are presented in [25], [26]. However, they provided a more general framework rather than focusing on lane change decision situations in particular.

The lane change trajectory is generated according to the vehicle state, surrounding vehicles and road information. Most of discussed researches either try to predict the behavior of surrounding vehicle or based on the kinematic functions and try to find an optimal trajectory or a safest path [27]–[29]. This paper is extended from our previous works [30], [31].

To exactly understand the human lane change model, we have conducted lane change experiments on expressways in Japan. The experimental data includes information about the human lane change behavior as well as the neighboring vehicles. By analyzing the human's behaviors from the experimental data, we realized that the human model was not a single stage but rather a two continuous-segment stage. Our work develops a lane change model based on a two-segment (behavior and motion) model, which accounts for lateral and longitudinal speed/spatial constraints that match the human drivers. A method to select the suitable behavior for longitudinal movement based on the  $dx/dv$  graph segmentation is proposed. This graph provides the safety distance  $dx$  and safety speed  $dv$  for doing the lane change based on the human-driver lane change patterns. At the “lateral segment,” the ego vehicle starts its lateral motion and enters into the destination lane. An optimization function is proposed which integrates both lateral and longitudinal trajectories in the same function. Through comparisons with the human-driver data, we found that the proposed evaluation function was able to select a motion (trajectory/path) close to the human-driver.

The main contributions of this paper are: I. We model the situation into an observation nine grid cell and introduce a classification of the grid state and corresponding available behaviors; II. We introduce an active/passive model based on the  $dv/dx$  graph. This model is intuitive and is modeled from the behavior model derived from the recorded-expert driver behavior in highway and it has very fast computation/evaluation time.

The structure of this paper is as follows; Section II explains the analysis of human lane change data and our proposed automated lane change flowchart. Section III introduces our two segments lane change model and behavior generation and selection criteria. The lane change motion planning is also described in section III. Section IV presents our simulation and comparison results. Finally, the conclusion is given in Section V.

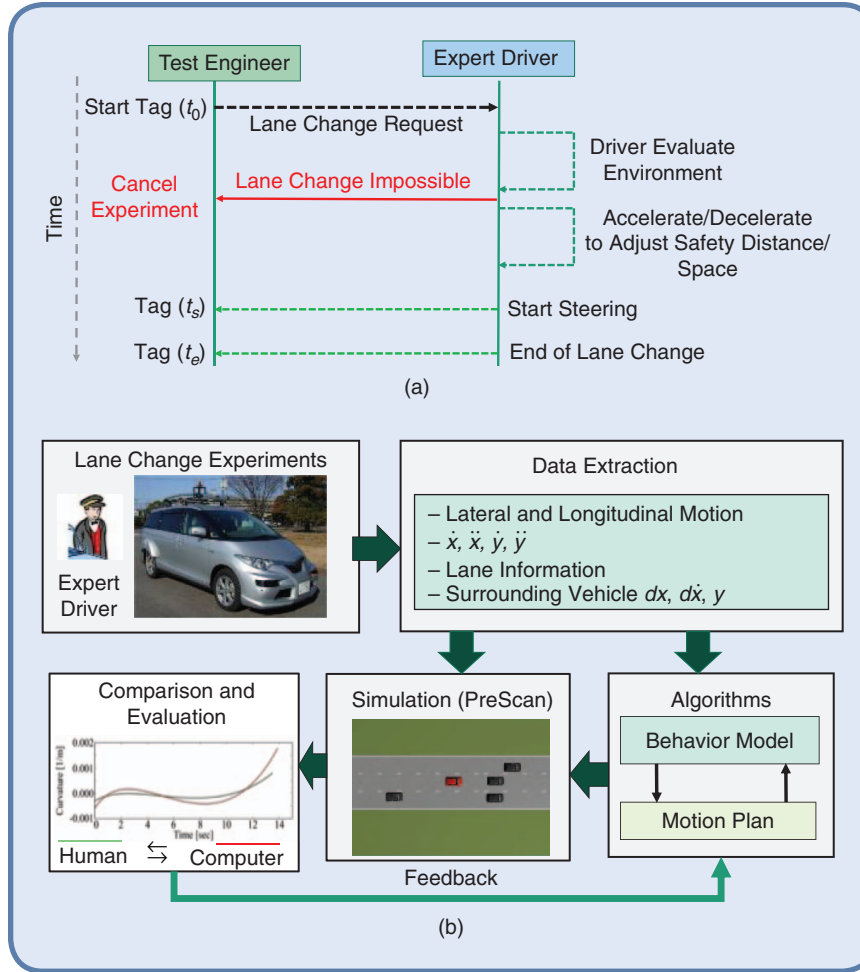


**FIG 1** Lane Change Experiment. (a) Lane change experiments process to extract the human driver behavior and (b) Lane change experiment diagram.

## II. Automated Lane Change Model

### A. Lane Change Experiment

The experiments were conducted at the Isewangan Expressway in Aichi prefecture, Japan. The experiment route had a length of 21.4 km. Different long-time-career expert drivers (whose driving skills are higher than average drivers) were selected for performing the lane change experiments. Lane change maneuvers were frequently performed between the different driving lanes to cover different scenarios in the expressway. The lane change experimental methodology utilized to record the human driver behavior and motion is shown in Fig. 1(a). As illustrated in Fig. 1(a), when the driver receives the request for changing the lane from the on-board test engineer, the driver adjusts the longitudinal speed (acceleration/deceleration) and finds a safe space and time instant to initiate the steering to perform the lane change. Lane change in the expressway is generally a challenging task, and the driver should adjust both the lateral

and longitudinal acceleration to perform safe and comfortable lane change. In the experiment, we also extracted the surrounding vehicles' information, including their relative distance, and speed. The acquired data was then analyzed to model the human driver behavior during the lane change. Figure 1(b) shows the diagram of the whole lane change experiment to extract data and evaluate the proposed lane change method.

### B. Lane Change Model

Through the lane change experiments, we observed that the human-driver lane change behavior model does not begin at the instant of the steering wheel turn, but rather a few seconds before the steering wheel turn. This is illustrated in Figure 2(a), where an example of a recorded lane change scenario is shown. The ego vehicle (red car) intends to change to the right lane. While observing the environment, the human driver perceives the presence of a vehicle ahead of the ego-vehicle in the current lane and another vehicle, coming from behind, in the intended target lane. In this scenario, as shown in sample in Fig. 2 (a), the human driver initiates the steering wheel turn at time

17, with the deceleration already initiated at time 0. The driver performs the deceleration from time 0 to time 15, and reduces the vehicle speed from 23.85 m/s to 22.23 m/s, before initiating the turn. The driver had to decelerate to maintain a safe space from the front vehicle in the current lane, and to wait for the vehicle coming from behind in the right lane to pass.

In this paper, a two-segment behavior/motion lane change model is proposed as shown in Fig. 2(b). In segment 1, which is termed as the “longitudinal segment,” the ego vehicle tries to adjust the longitudinal distance, position or relative velocity to make or find the suitable free space both in front of it and in the destination lane. In segment 2, termed as the “lateral segment,” the ego vehicle starts the lateral motion and enters into the destination lane. The driver behavior in segment 1 is highly dependent on the number of surrounding vehicles, the ego vehicle-surrounding vehicle distance and their relative velocities. Additionally, the time and distance information of the surrounding vehicles entry or exit from an

adjacent lane to the current lane is also taken into consideration. Finally, in scenarios, where the surrounding vehicle either merges or exits the expressway, apart from the distance and time considerations, the length of the merging and exit lanes are taken into consideration. There are also other important parameters such as road curvature, visibility conditions or behavior of the surrounding vehicles. By analyzing different cases of human lane change data, the following behaviors for the segment 1 are extracted.

$$B = \int \left\{ \begin{array}{l} \text{do lane change(LC), passive(wait),} \\ \text{active(accelerate), active(decelerate),} \\ \text{active(evasive)} \end{array} \right\} \quad (1)$$

Although it is difficult to develop a general behavior model, it is possible to propose a standard model that guarantees the safety and smoothness of the lane change operation. For example, if there is enough space in the destination lane, the vehicle can turn the steering wheel and **do the lane change**. If the relative speed of the approaching vehicles in the destination lane is relatively high, ego vehicle may prefer to **wait (passive)** until finding enough free space. In this case, it may even do **deceleration (active)** to reduce the time or traveled distance. The deceleration behavior may be useful in the case of time/distance constraint when ego vehicle has to change the lane to exit from the expressway. In the other case, when the relative speed of the neighboring vehicles in the destination lane is relatively low, ego vehicle may **accelerate (active)** to pass the neighboring vehicles for doing the lane change. If there is a sudden change in the behavior of the surrounding vehicles during the lane change (sudden acceleration, deceleration or lane change), ego vehicle might need **evasive (active)** maneuver to avoid accident.

### C. Automated Lane Change Flowchart

Automated lane change is an integration of sensing/perception, planning (behavior & motion) and control. The behavior/motion flowchart for performing the lane change is shown in Fig. 3. It starts with the estimation of motion parameters/position of neighboring vehicles to estimate their trajectories. Based on the driving lane information and the behavior/motion parameters of the neighboring vehicles, a trajectory for a certain period [0~T] can be estimated. By using the trajectory data points ( $t, x(t), y(t)$ ), the occupancy grid map of the current and future states of the surrounding environment are estimated. In the subsequent section, the main components of the automated lane change flowchart are briefly explained.

### D. Situation Modeling

The current lane change situation is modelled into a state occupancy grid as in the Fig. 4. This state grid is attached

to the vehicle position. The grid cell's width and orientation are equal to the lane width. The middle cell length  $d_{ego}$  is equal to the ego vehicle length plus a safety distance. The grid's size is calculated based on the relative velocity of the ego vehicle and surrounding vehicles, and the time to complete the lane change. The front cell size's

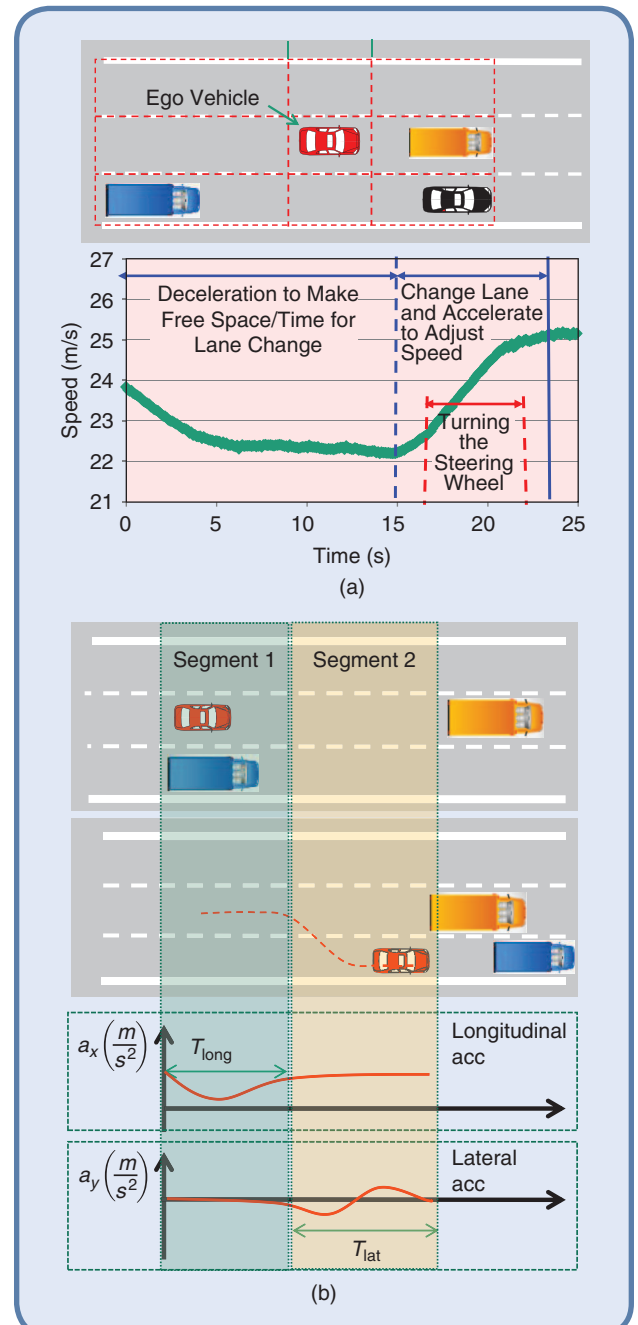


**FIG 2** Two-segment lane change model. a) An example lane change scenario. ego vehicle (red car) wanted to change to the right lane. There was one vehicle ahead of the ego-vehicle and one vehicle coming from behind in the intended target lane and (b) “Longitudinal” segment adjusts the relative velocity to find suitable free space in front of it and in the destination lane. “Lateral segment” adjusts lateral steering motion and enters the destination lane.

$d_{front}$  is calculated based on the closest vehicle in the front, and behind cell's size  $d_{back}$  is calculated based on the corresponding closest vehicle approaching from behind.

$$d_{front} = d_{min} + \max\{v_{ego} - v_{front}, 0\} * Time_{LC} \quad (2)$$

$$d_{back} = d'_{min} + \max\{v_{back} - v_{ego}, 0\} * Time_{LC} \quad (3)$$

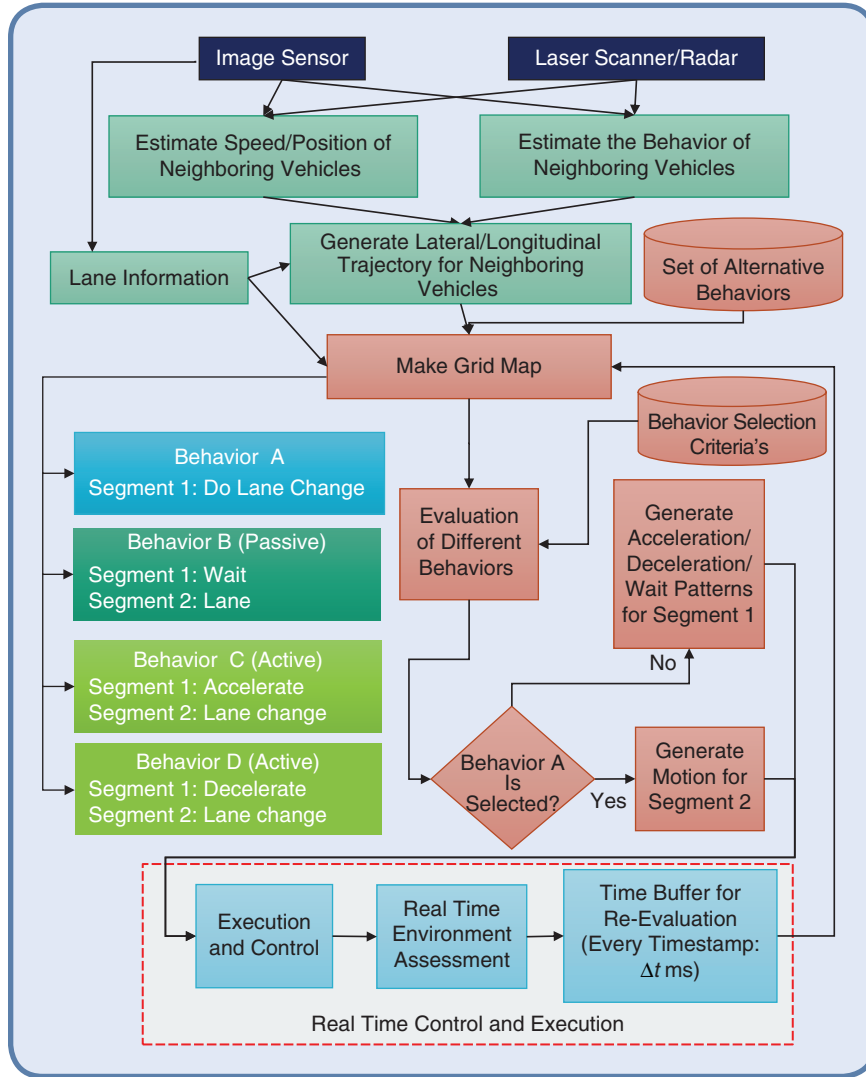


FIG 3 Automated lane change flowchart.

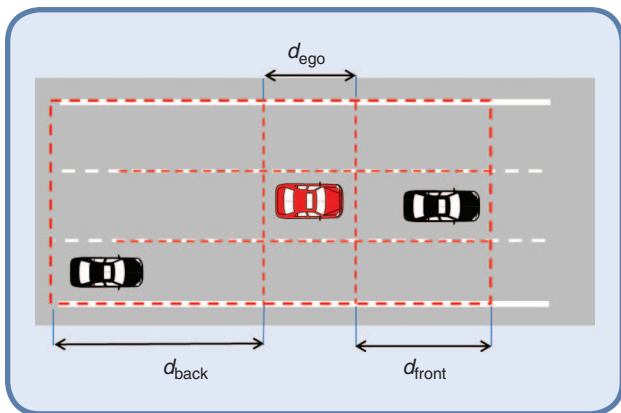


FIG 4 Environment grid modelling.

$Time_{LC}$  is the intended or required time to perform the lane change maneuver, and it takes 4–6 s for a typical driver to complete the lane change, based on the human driver data [32].  $v_{front}$  is the velocity of the closest vehicle in the front, and  $v_{back}$  is the velocity of the closest vehicle behind the ego vehicle;  $d_{min}$  and  $d'_{min}$  are the human defined minimum safety distances;  $v_{ego}$  is the current ego vehicle's velocity. In literature, the grid cells are generally considered to be same size [5], [8]. In this article, through empirical simulations and recorded human-driver data, we realized that the center cells in the grid were dependent on the vehicle size alone and were generally smaller than the front and back cells in the grid. A larger size for the center cell causes the ego vehicle to refrain from performing the lane change due to the occupation of the center cells in the left or right side. We also realized that the back cells have to be larger compared to front cells, in order to mimic the human behavior.

Each cell in our discretized nine-cell environmental grid, is represented by a state. Typically, there are eight surrounding cells in the occupancy grid and each cell can be either free (cell value = 0) or occupied (cell value = 1). Thus there are totally  $2^8 = 256$  states. However, the vehicle only performs either the left side or right side lane change maneuver at a given time. In this scenario, the three cell's belonging to the opposite side of the decided lane change can be temporarily ignored so that the number of state can be reduced to  $2^5 = 32$  states. These 32 states include the scenario when another vehicle “cuts-in” from the neighboring lane. In this scenario, the state of the front grid cell will be changed to occupied, which will influence the longitudinal control behavior in the intended lane change.

#### E. Trajectory Estimation of Neighboring Vehicles

As shown in Fig. 5, the trajectory of a neighboring vehicle is estimated from the recorded position data and the lane

center point. Assuming that this vehicle will follow the center of the lane, a quantic polynomial curve is fitted to these data. This is given as

$$y(t) = a_5 t^5 + a_4 t^4 + a_3 t^3 + a_2 t^2 + a_1 t + a_0 \quad (4)$$

$a_i (i = [1, 4])$  is polynomial function's factor which can be calculated based on the past motion data point and the lane center points. Since the data is derived from the surrounding vehicle's past motion data and center-lane points, the generated polynomial curves/trajectories will stay in lanes.

In Fig 5,  $T_{\text{hist}}$  is the recorded time and  $T_{\text{opr}}$  is total operation/prediction time. Here, “Frenet Frame” method is applied in order to combine different lateral and longitudinal motions in one equation [33]. In this case, the lateral and longitudinal motion of each vehicle can be presented by an equation which is based on the distance traveled along the center line. There are effective collisions checking methods in the literature to check the collision between two trajectories [34]. To check the collision in the simulation platform, the trajectory of the neighboring vehicle is sampled for a certain period [0~T]. In this article, the Inevitable Collision States (ICS) method [35] is applied to check the collision possibility between two trajectories.

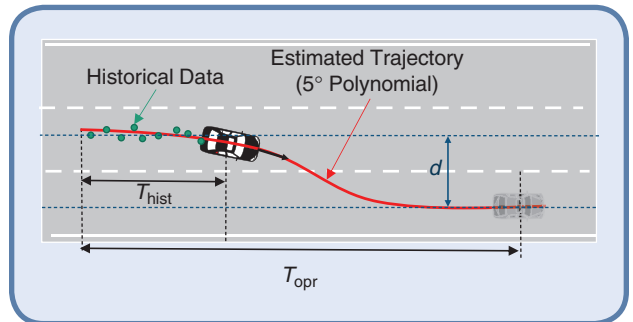


FIG 5 Neighboring vehicle's trajectory estimation.

### III. Behavior and Motion Generation

#### A. Situation and Behavior Assessment

For every state, different alternative behaviors are considered as shown in Fig. 6. For the situation in Fig. 6, different following behaviors are available to do the lane change;

- Behavior A: The ego vehicle does the lane change with current speed as there is enough space and the relative velocities of the vehicles in the right lane are not high.

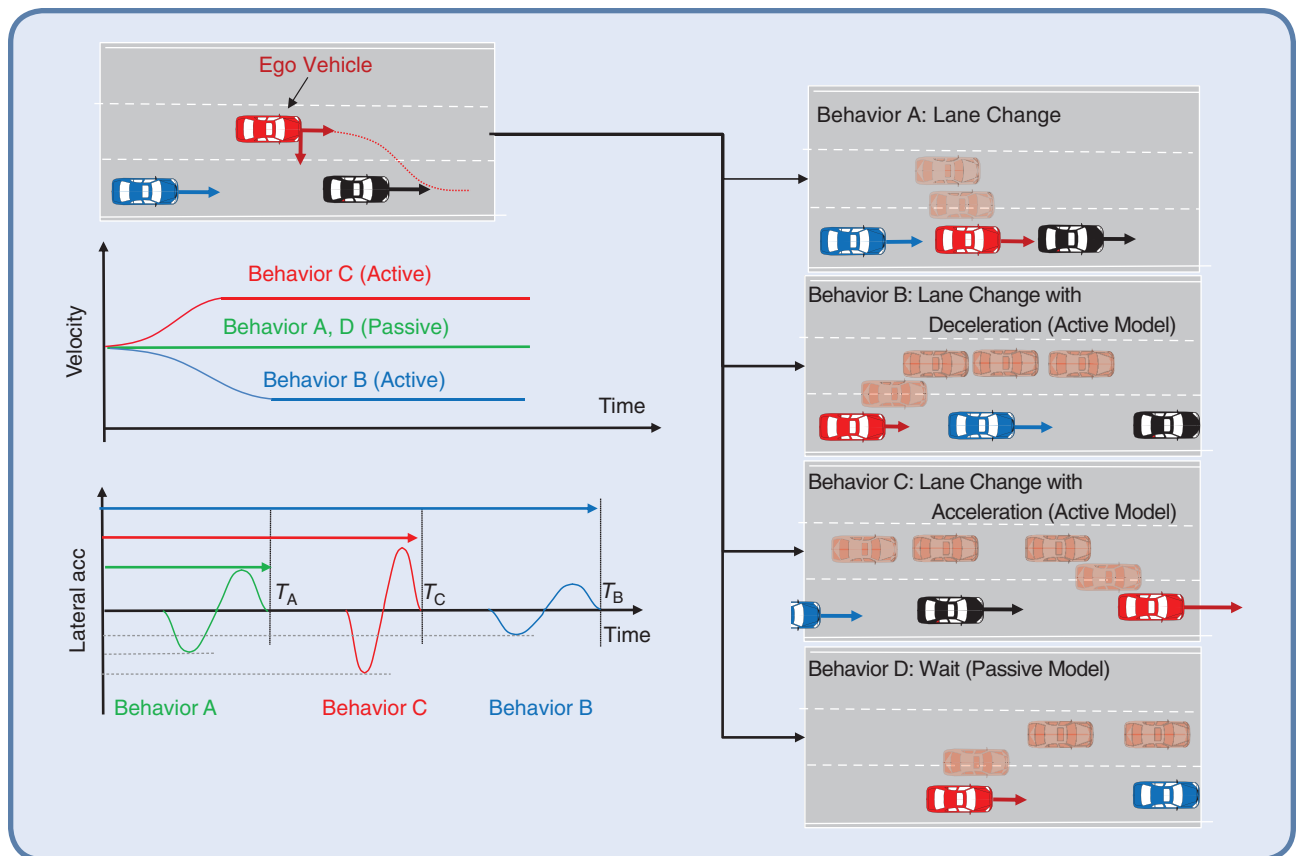


FIG 6 Different available behavior and motion for lane change and velocity profile corresponding to each behavior.

An intuitive method to extract the behavior patterns from the human-driver recorded data is proposed. For this purpose, we use the observation grid to estimate the current situation.

- Behavior B (active): The ego vehicle decelerates and enters to the right lane at the back of the vehicles. It is preferable behavior when the lane change at limited time/distance has to be done (for example exit point in the expressway).
- Behavior C (active): The ego vehicle accelerates and enters to the right lane at the front of vehicles.
- Behavior D (passive): If the relative speeds of right lane vehicles are high, the ego vehicle just waits until the right lane vehicles passes and the right lane becomes free to do right lane change.

The proper behavior can be selected based on the relative distance and between the ego vehicle and neighboring vehicles. The large differences in the relative velocity are shown in the graph, in Fig. 6, which was extracted from recorded human-data. To have an exact understanding of different behaviors, we categorized the 32 ( $2^5$ ) occupancy grid states (left or right lane change) to the following four main categories. The behavior alternatives are limited to the categories that reduce the calculation time. The different categories for the occupancy grid states are shown in Fig. 7. In Fig. 7, the white cells are empty cells, light gray cells are the omitted cells and black cells are occupied cells. The categories and alternative behaviors are defined by analyzing the human-driver data for different lane change scenarios.

- **Category A:** There are two alternative behaviors for occupancy grid states. The ego vehicle either waits or performs the lane change based on the relative speed and distance to the neighboring vehicles.
- **Category B:** There are more alternative behaviors for states in this category. The ego vehicle may do the lane change but sometimes acceleration/deceleration or wait is preferable to do safer/smooth lane change. In the case of time/distance constraint, acceleration/deceleration may be necessary to satisfy the lane change limitations.
- **Category C:** It is related to complicated state during lane change. In this category, the right cell of the ego vehicle is occupied and suitable behavior should be selected to provide free space in the destination lane. Ego vehicle may accelerate, decelerate or wait for states in this category.
- **Category D:** The ego vehicle has to wait for doing the lane change and any other behavior may be dangerous.

The observation grid state can transit from one category to another depending on the driver and neighboring vehicles. The human driver often maps the current situation in his brain and matches it with the four categories and predicts the future scenario, if a specific behavior is selected. Eventually, category A is selected by accelerating or decelerating the vehicle, and lane change maneuver is initiated.

### B. Behavior Selection

To select the suitable behavior for lane changing, there are many researches in the literature that are mainly based on HMM [36] or Bayesian network [27]. In this section, an intuitive method to extract the behavior patterns from the human-driver recorded data is proposed. As mentioned in section II.D, we use the observation grid to estimate the current situation. The grid's length reflects the vehicle speed (the higher speed the longer the grid). When the grid related cells in the destination lane are empty then it is possible for lane change as in Fig. 7. The  $dx/dv$  graph shows the human-driver's behavior selection in highway when there is more than one available behavior. This graph corresponds to the "longitudinal segment" in proposed lane change model. The  $dx/dv$  graph is drawn for all the recorded lane change data from start  $t_0$  until end of the lane change at  $t_e$ . Each draw includes the  $(dx, dv)$  status for the "longitudinal segment," while the driver adjusts the longitudinal distance/speed to generate a safe space and time before the steering at  $t_s$ . An example of  $dx/dv$  for human driver regarding to a typical right lane change scenario is shown in Fig. 8. The horizontal axis is the related distance  $dx$  between vehicle in the target lane and the ego vehicle, and vertical axis is the velocity difference  $dv$  between two vehicles. In Fig. 8, the human driver slowly accelerates (active) until the neighboring vehicle in the right lane passes.  $(dx, dv)$  points are shown in Fig 8. These points are noisy, which can be attributed to the sensor noise and detection/tracking uncertainties. As a result, the  $(dx, dv)$  points are not smooth or linearly continuous. To handle the sensor uncertainty and noise, we consider a margin for the  $(dx, dv)$  data and interpolate a line to model the human driver behavior.

The  $dx/dv$  graph for right lane change cases is shown in Fig. 9. The horizontal axis is the distance between vehicle in the target lane and the ego vehicle, and vertical axis is the relative velocity between the two vehicles. The lines show different recorded right lane change data that start from  $t_0$  (human-driver decide to do the right lane change) until the  $t_s$  (red star) that driver steers to enter the right lane and continue. Based on the different samples of human-driver that are shown in Fig. 9, the  $dx/dv$  graph's area

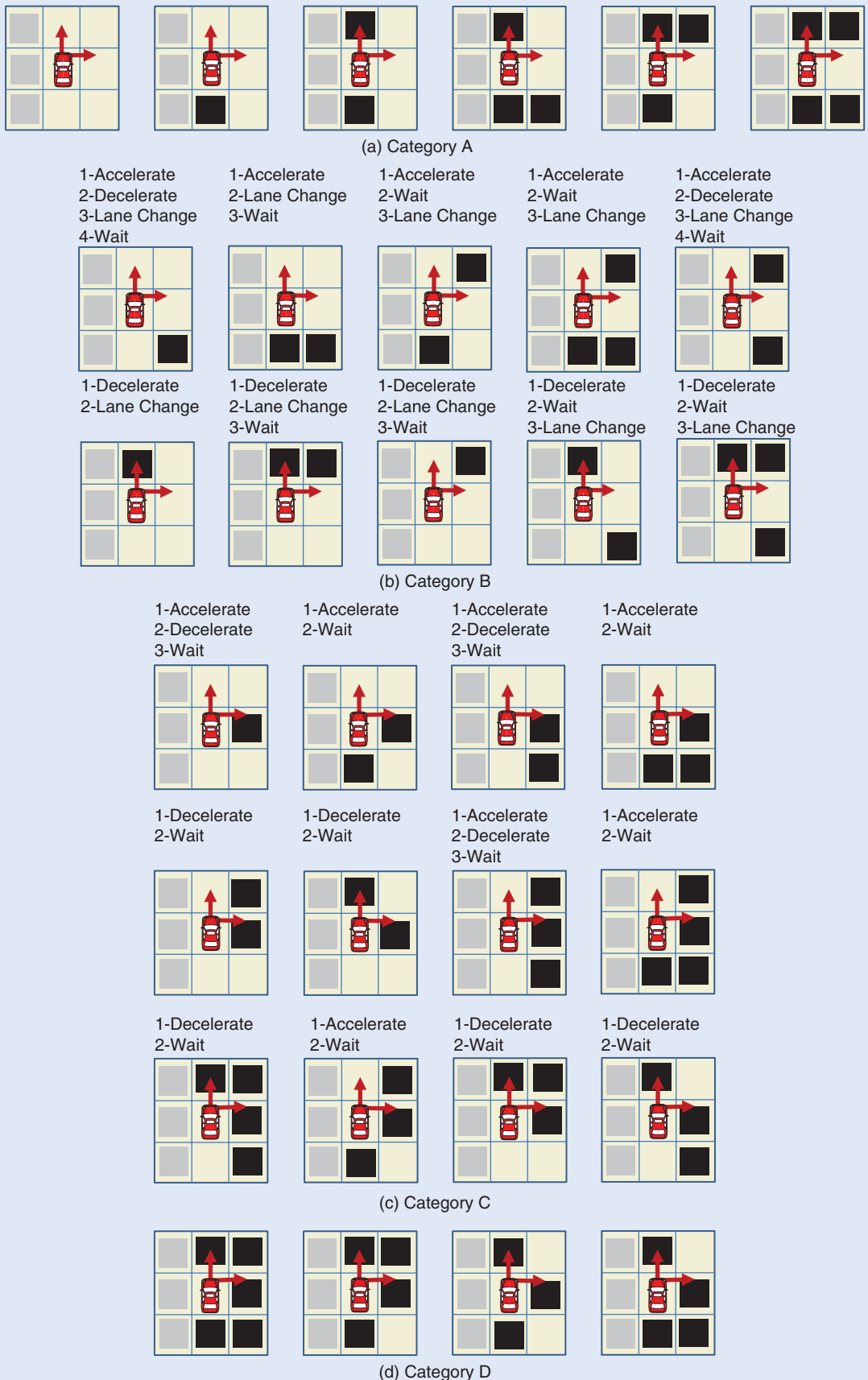


**FIG 7** All 32 states models for right lane change and available alternative behaviors for each of them.

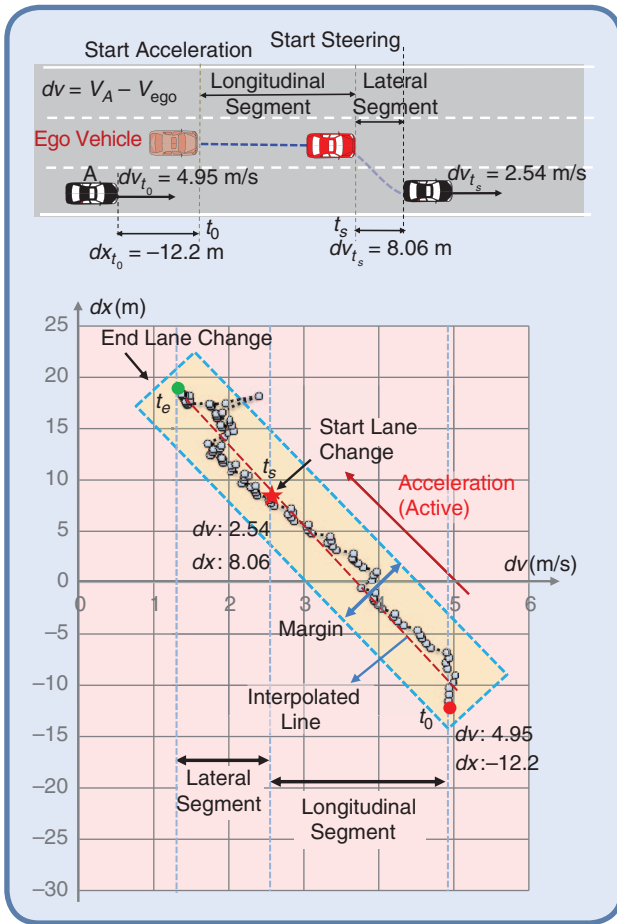


FIG 8  $dx/dv$  graph for human right lane change.

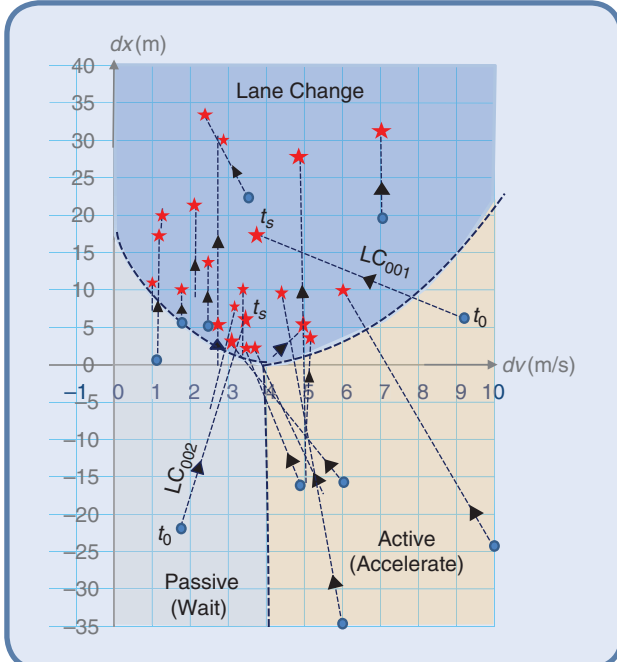


FIG 9  $dx/dv$  graph related to human driver behavior for doing the right lane change.

is divided into three areas corresponding to three different behaviors including *lane change*, *accelerate (active)* and *wait (passive)* based on the initial value for  $(dx, dv)$ . The curves between lane change and other sections are the non-linear classification boundary (the hyperplane) after training the data by the support vector machine method using the radian basis function (RBF):

$$e^{-\gamma||a-b||^2} \quad (5)$$

where  $a$  and  $b$  are input training data and  $\gamma = 0.01$  is human set value. The resulted of RBF-SVM training is a nonlinear decision boundary when projected into 2D space, this boundary often has the form of a curve. In Fig. 9, only the decision boundary which is close to the data set is shown.

At the start of the right lane change, if the corresponding  $(dx, dv)$  point is in the “Lane Change” area, the ego vehicle is able to enter to right lane. If the  $(dx, dv)$  is in the “Wait” (passive) area, ego vehicle waits until  $(dx, dv)$  enters the “Lane Change” area (the right vehicle pass) and then enters to the right lane. If the  $(dx, dv)$  is in “Accelerate” (active) area, ego vehicle will accelerate and wait until  $(dx, dv)$  value enters the “Lane Change” and then do the lane change. The acceleration behavior is usual because the ego vehicle enters the higher speed lane and it should adjust speed with current lane. This graph also shows the safety relative distance  $dx$  or relative speed  $dv$  for doing the safe and comfortable right lane change. For sample  $LC_{001}$  in Fig. 9, the driver accelerates and reduces its relative speed before entering the right lane. For sample  $LC_{002}$ ,

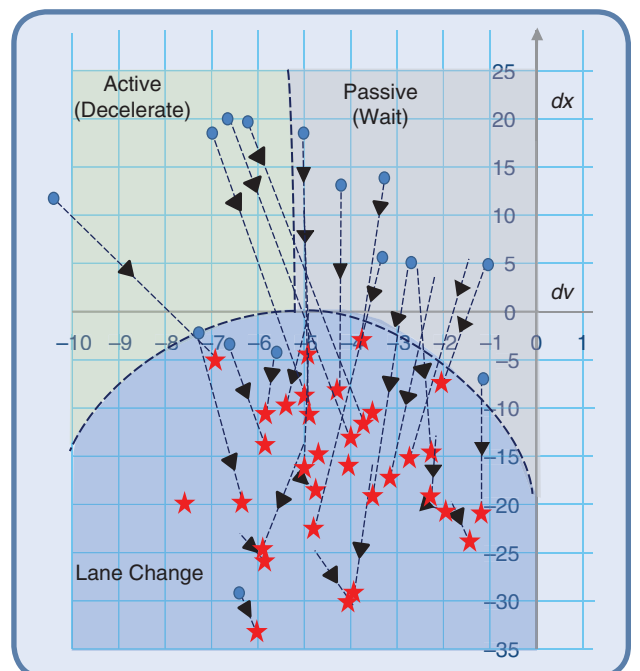


FIG 10  $dx/dv$  graph related to human driver behavior for doing the left lane change scenario.

the driver waits until the right lane vehicle passes it and then starts to enter to the lane change.

The  $dx/dv$  graph in Fig. 9, is only prepared for the positive values of  $dv$  because all the human lane change data lie in this area and vehicles in the right lane have generally higher speed. To complete the graph and cover all the values of  $dv$ , it is necessary to provide the human driver lane change data for the negative values of  $dv$ .

The  $dx/dv$  graph for the typical left lane change cases in expressway was also prepared. As shown in Fig. 10, the driver behavior is different from the right lane change because in this case, the vehicle enters to the lower speed lane.

As shown in Fig. 11, there is a vehicle in the right lane and we are initiating the right lane change with initial condition at  $(dx_{t_0}, dv_{t_0})$ . There are many alternatives as shown by different lines from No. 1 to No. 5 for doing the lane change. For example, in case No.1, we just decrease (active model) ego vehicle's speed until the back vehicle in the right lane passes.

In Fig. 9, there is an area, where most of the human lane change begins; we named this area as the “most preferable area.” This area is generated based on 3-class support vector machine classification and Gaussian estimation of the lane change start points. In the “most preferable area,” the relative velocities  $dv$  is between  $[0 \sim 3 \text{ m/s}]$  and relative distance  $dx$  is between  $[5 \sim 20 \text{ m}]$ . To select the human like behavior for doing the right lane change, we draw the shortest line from initial condition at  $(dx_{t_0}, dv_{t_0})$  to “most preferable area” and generate speed profile and lane change timing. We track the  $(dx, dv)$  and when we enter “most preferable area,” we start to do the lane change. One advantage of our approach in comparison with other related method is the calculation time. Since all the data are recorded and processed off-line to generate the  $dv-dx$  graph. The behavior selection is simplified into matching the current  $(dv-dv)$  point into the graph so that the calculation time is small (less than 10 ms).

### C. Longitudinal Velocity Profile

According to the active/passive behavior, the corresponding desired vehicle's velocity profile is calculated. The acceleration/deceleration patterns are presented in the form of a function of ego vehicle position, velocity and the target leading/behind vehicle.

Fig. 12 illustrates the vehicle acceleration behavior when a leading vehicle exists in the neighboring lane. In this scenario, ego vehicle accelerates and passes the leading vehicle. The acceleration is continued till sufficient safe distance is achieved, before performing the lane

One advantage of our approach in comparison with other related method is the calculation time, since all the data are recorded and processed off-line to generate the  $dv-dx$  graph.

change maneuver. The ego vehicle's acceleration is calculated based on (6):

$$\ddot{x} = \frac{2(x_{\text{lead}}(t_0) - x(t_0) + T(v_{\text{lead}}(t_0) - v(t_0)) + r)}{T^2} \quad (6)$$

where  $x(t_0)$ : vehicle position at time  $t_0$ ;

$v(t_0)$ : velocity at time  $t_0$ ;

$x_{\text{lead}}(t_0)$ : leading vehicle position at time  $t_0$ ;

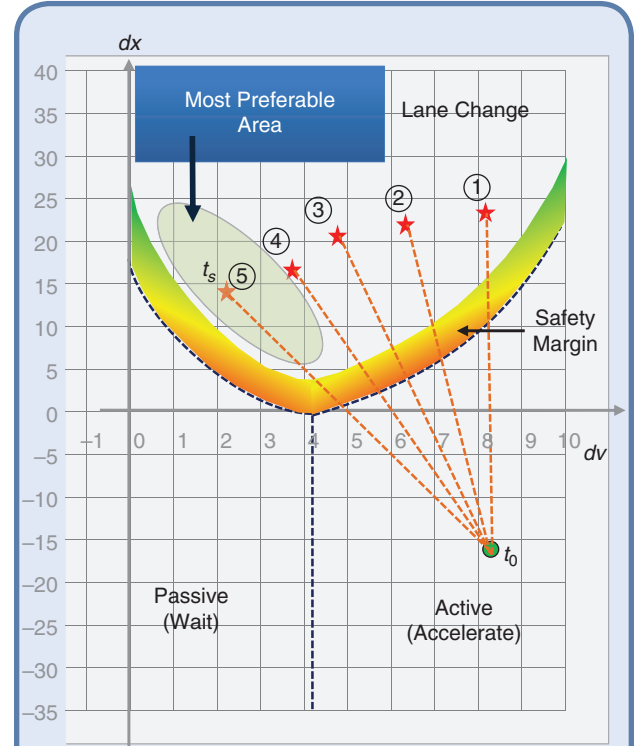


FIG 11 Selection of suitable behavior pattern based on the initial value of  $(dv, dx)$  for right lane change.

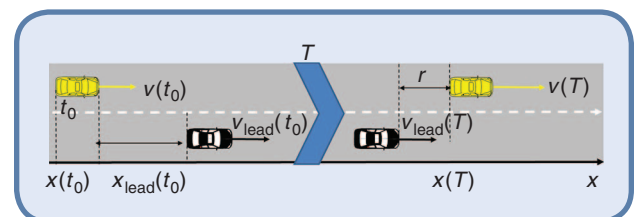


FIG 12 Vehicle acceleration for passing.

$v_{\text{lead}}(t_0)$ : leading vehicle position at time  $t_0$ ;  
 $T$ : operation time horizon;  
 $r$ : safety reserving distance;  
 $r$  is calculated through leading vehicle velocity and time to react  $TTR$

$$r = d_{\min} + v_{\text{lead}}(T) * TTR \quad (7)$$

To generate smooth and comfort acceleration/deceleration motion, the following cost function is minimized;

$$\int_0^T (w_{\text{dist}} [\Delta d(t)]^2 + w_{\text{acc}} [\ddot{x}(t)]^2) dt \quad (8)$$

where  $w_{\text{dist}}$  and  $w_{\text{acc}}$  are human given weighted factor to balance between the jerk and safety distance ( $\Delta d$ ). This cost function is similar to the method presented in [20] though the operation time  $T$  is fixed in [20]. In our approach, the operation time  $T$  is not fixed to have more degree of freedom. The error in the safety distance ( $\Delta d(t)$ ) is calculated by the following;

$$\Delta d(t) = x_{\text{lead}}(t) - r + t * \dot{x}_{\text{lead}}(t) - x(t) \quad (9)$$

There is direct method to solve the above problem using Lagrange multiplier and Gradient Descent. Though finding the exact solution for optimization problem in (8) is difficult and time consuming. Here, we turn our attention to approximations of the minimizer through a simplification and sampling from search space. Instead of calculating the

best trajectory explicitly and modifying the coefficients to get a valid alternative, we generate in a first step, such as in [33], [38], alternative trajectories for both  $x(t)$ ,  $y(t)$ . Later we can pick the valid and safe motion which is safe and has the lowest cost value.

The quartic polynomial function is utilized to generate acceleration/deceleration motion [34].

$$x(t) = b_4 t^4 + b_3 t^3 + b_2 t^2 + b_1 t + b_0 \quad (10)$$

The coefficients  $b_i (i = [1, 4])$  are estimated by considering ego vehicle constraints (maximum acceleration/deceleration and speed), operation time ( $T$ ) and desired velocity at the end  $\dot{x}(T)$ . Alternative longitudinal trajectories are generated by sampling a valid range of operation time  $T$  and final velocity  $\dot{x}(T)$  (it can be extracted from  $dx/dv$  graphs) while considering the boundary conditions including maximum and minimum acceleration  $\ddot{x}_{\max}, \ddot{x}_{\min}$ . We generate alternative speed profiles by sampling and select the best speed profile which has the lowest value for cost function in (8).

#### D. Lateral trajectory

To model a lateral trajectory during a lane change, many approaches in literature use the 5th degree polynomials as it provides minimum jerk for steering [27], [37]. Polynomial function provides a geometric modelling of the vehicle trajectory that responds to the realistic demands of the lane change maneuver.

$$y(t) = a_5 t^5 + a_4 t^4 + a_3 t^3 + a_2 t^2 + a_1 t + a_0 \quad (11)$$

The equation coefficients  $a_i (i = \overline{0, 4})$  are calculated considering dynamic constraints (boundary conditions for lateral acceleration) and values of the position, velocity and acceleration at initial and endpoint. The initial velocity and acceleration of the vehicle can be obtained from the CAN. These values can be used to generate the alternative lateral trajectories by changing operation at time  $T$ .  $T$  is sampled from a valid range of operation time and ending conditions to generate alternative lateral trajectories while considering the boundary conditions including  $\ddot{y}_{\max}, \ddot{y}_{\min}$  and  $\kappa(t) \leq (\dot{y}_{\max}/\dot{x}(t))^2$  to avoid slip. The best lateral motion is selected which minimize the following cost function that includes lateral jerk, heading error and smoothness;

$$J = w_{\text{jerk}} \int_0^T \ddot{y}^2(t) dt + w_{\text{heading}} [\kappa(T) - \kappa_{\text{road}}]^2 + w_{\text{smoothness}} \int_0^T \frac{\dot{k}(t)^2}{\sqrt{\dot{x}(t)^2 + \dot{y}(t)^2}} dt \quad (12)$$

where  $w_{\text{jerk}}$ ,  $w_{\text{heading}}$  and  $w_{\text{smoothness}}$  are human given weighted factors.

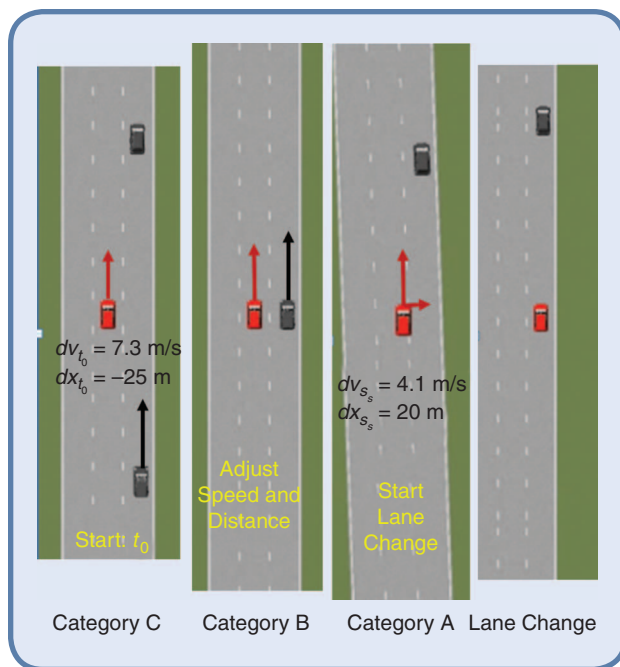


FIG 13 Automated right lane change simulation.

## IV. Simulation

To evaluate and test the proposed model, a simulation platform on the Prescan was developed. It includes different modules for sensing, behavior/motion planning, trajectory estimation of neighboring vehicles and ego vehicle's control. The behavior/motion generation module is developed under C++ to increase the efficiency of the simulation platform.

### A. Lane Change Scenario

Fig. 13 shows simulation results for the right lane change scenario with different relative speed ( $dv$ ) for neighboring vehicles (ego vehicle is red one and it is going to do right lane change). In Fig. 13, the ego vehicle (red vehicle in the central lane) wants to perform the lane change maneuver to the right-side lane with initial ( $dx_{t_0} = -25$  m,  $dv_{t_0} = 7.3$  m/s). Based on the proposed method, the ego vehicle makes a speed and timing profile to the “most preferable area” as shown by dotted red line in Fig. 14. It slowly accelerates (active model) and starts the lane change when enter to the safe area as shown in Fig. 15 simulation. We have tested the proposed method with different initial ( $dx_{t_0}, dv_{t_0}$ ) and the results are shown by dotted lines in Fig. 14. The tested results show that the proposed model works properly, without any collision during the lane change simulation.

### B. Merge and Exit

The proposed  $dx/dv$  model was extended to cover more complicated cases of lane change for merging into traffic highway. In these cases, the time/distance for doing lane change is limited. The suitable behaviors for merge and exit are active model (*accelerate or decelerate*) to do the lane change as soon as possible. The proposed  $dx/dv$  segments and suitable behavior for each segment is shown in Fig. 15. Two simulations to exit or merge (Fig. 16 and Fig. 17) which consider two initial statuses for ( $dv, dx$ ) are shown by  $LC_{01}, \dots, LC_{04}$  in Fig. 16. For  $LC_{02}$  and  $LC_{04}$ , the values of ( $dv, dx$ ) fall in the accelerate area and the acceleration behavior is selected to merge the expressway. For  $LC_{01}$  and  $LC_{03}$ , the values of ( $dv, dx$ ) fall in the deceleration area and the suitable behavior is decelerate to merge the expressway. As shown in Fig. 15, the  $dx/dv$  changes are not linear like normal lane changes and there are sharp changes in the  $dv$  (accelerate and decelerate) to enter the lane change area in shorter time. The simulation results for  $LC_{01}$ ,  $LC_{04}$  are shown in the Fig. 16 and Fig. 17 respectively.

Simulations to exit the expressway are also carried out. Two examples which considering two initial statuses that are shown by  $LC_{01}$ ,  $LC_{03}$  in Fig. 15. In these case, there are also sharp changes in the  $dv$  (accelerate and decelerate) to enter the lane change area in shorter time. Based on the position in a prior known (or recorded global map), the

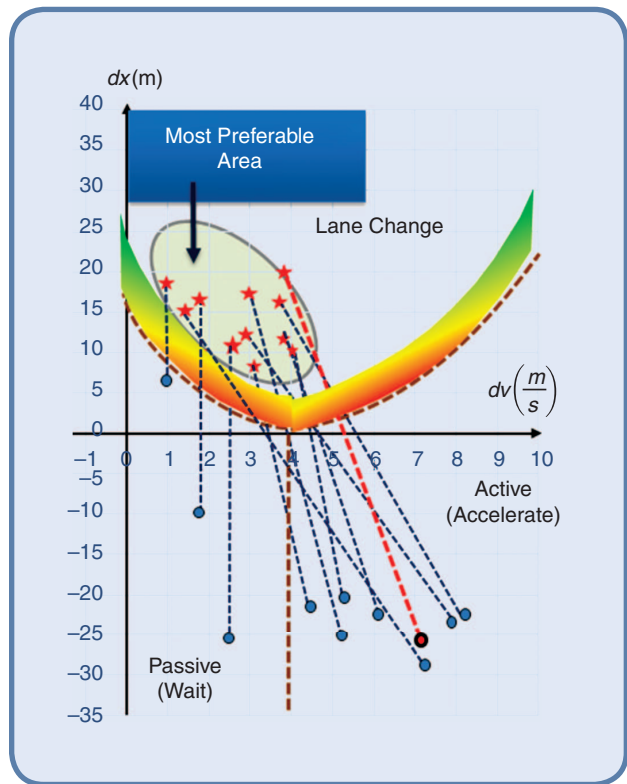


FIG 14  $dx/dv$  graph related to simulated right lane change.

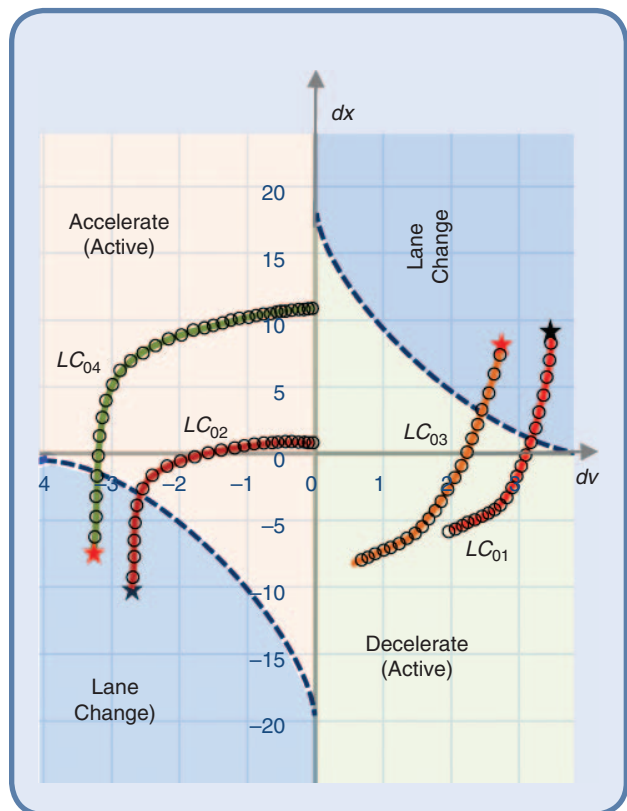


FIG 15  $dx/dv$  graph for right lane change simulation scenarios.

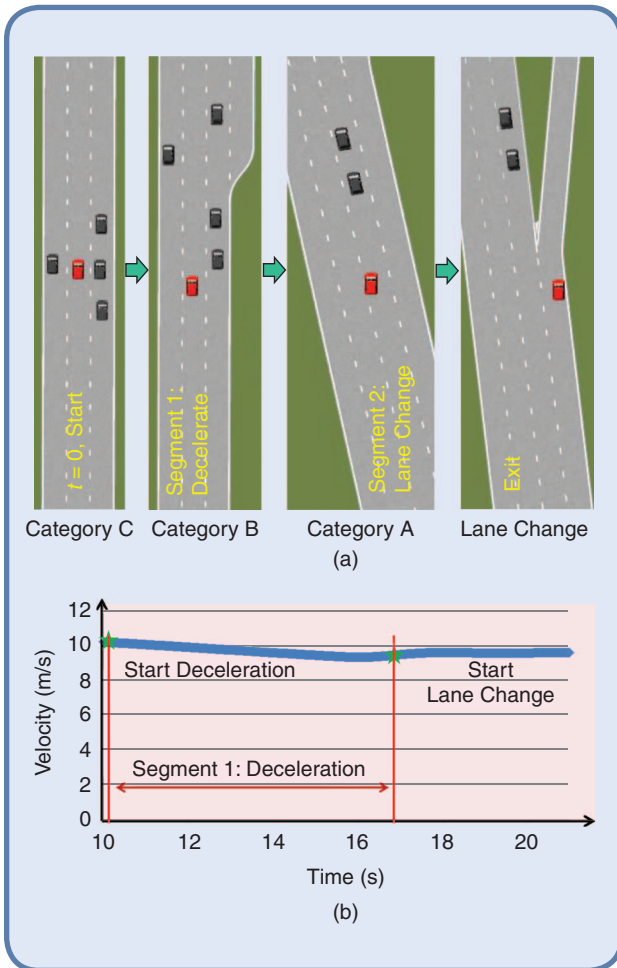


FIG 16 Simulation results to exit from highway for  $LC_{01}$ . (a)  $LC_{01}$ , exit from expressway simulation -deceleration and (b) Velocity profile to exit from expressway for  $LC_{01}$ .

ego vehicle is able to know if it is close to the merge or exit position or not. The system is then able to decide between patterns in Fig. 9 or Fig. 15.

### C. Comparison between Human and Computer

In our method, we “mimic” the human driver in “longitudinal segment,” however, in “lateral segment,” we applied polynomial functions to generate lane change trajectory. In this section, we compare human-driver with computer motion generator for “lateral segment” during the expressway lane change. To evaluate both lateral and longitudinal trajectories in same function, the lateral jerk and smoothness are utilized as Kanayama and Hartman proposed [37]. Evaluation function is defined as integral over the square of arc-length derivative of curvature along the path for a function  $f(x)$  with curvature  $\kappa(x)$ . The results of comparison between human-driver and computer motion generation for lateral segment are shown in Table 1. In most cases the computer can generate close or even better

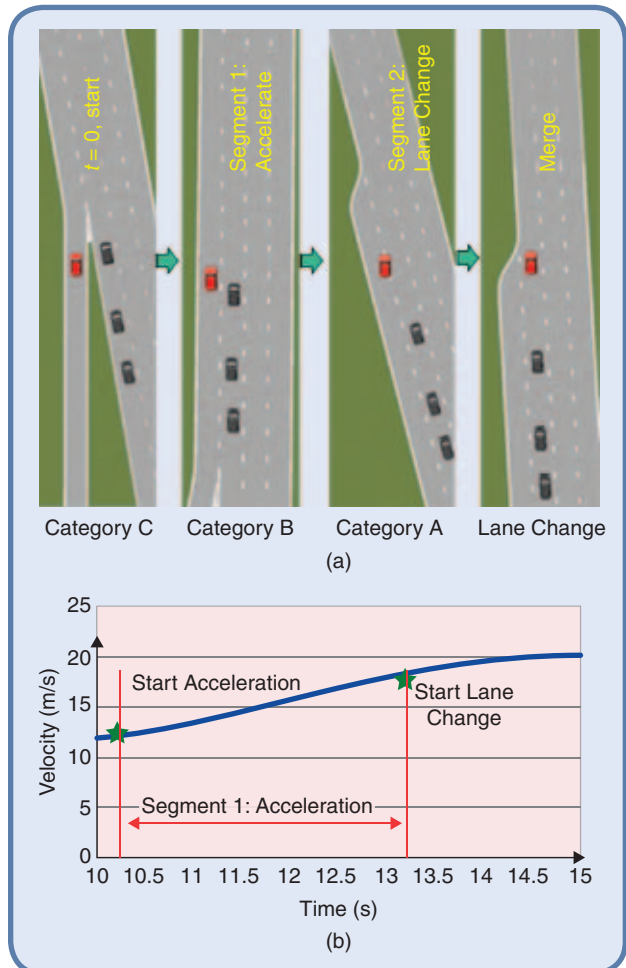


FIG 17 Simulation results to merge in expressway. (a) merge in expressway simulation acceleration behavior and (b) Velocity profile to merge in expressway.

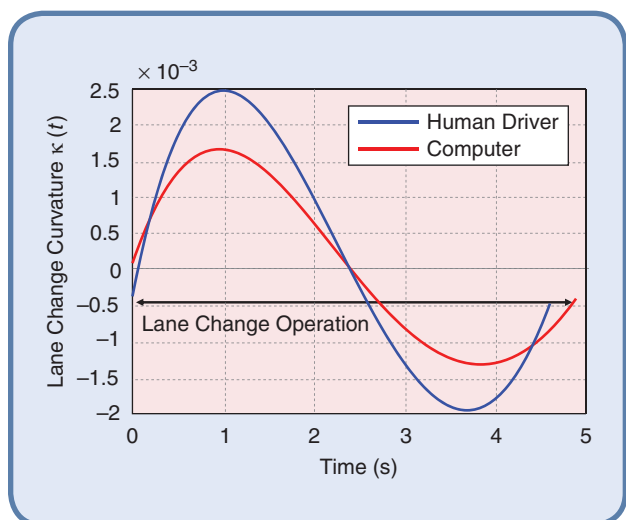


FIG 18 Human-driver and computer curvature  $\kappa(t)$  over time for lane change- blue curve shows smoothed IMU data from driver, red curve shows the computer.

Table 1. Computer and human driver analysis for lane change data.

Case	Operation Time - $\Delta t(s)$		Smoothness $^{-1}$		Lateral Jerk	
	Human-Driver	Computer	Human-Driver	Computer	Human-Driver	Computer
1	4.92	5.075	1.23E-07	1.19E-07	0.746	0.761
2	7.135	7.175	1.12E-06	7.35E-07	0.810	0.802
3	4.195	4.06	8.35E-07	6.12E-07	1.280	1.145
4	4.265	4.22	4.00E-07	2.93E-07	2.275	2.102
5	4.15	4.17	7.34E-07	4.91E-07	0.432	0.303
6	3.66	3.705	3.10E-07	1.89E-07	1.306	1.022
7	3.02	3.075	9.70E-08	6.48E-08	0.229	0.199
8	3.995	4.04	3.19E-07	2.02E-07	1.049	0.863
9	5.605	5.6	8.94E-07	6.69E-07	1.859	1.463
10	4.285	4.315	3.94E-08	2.09E-08	0.351	0.205
11	3.195	3.18	2.37E-07	1.18E-07	0.334	0.242
12	3.025	3.02	3.09E-06	3.14E-06	6.611	8.112
13	4.83	4.965	3.22E-07	6.32E-08	0.573	0.130
14	3.85	4.1	1.46E-06	1.04E-06	4.226	3.823
15	4.585	4.665	2.62E-06	3.01E-06	10.156	12.169
16	5.155	4.96	1.23E-07	8.44E-08	0.760	0.597
17	4.335	4.545	1.79E-07	4.50E-08	0.473	0.205
18	4.425	4.375	1.01E-07	3.61E-08	0.475	0.186

motion sets compared to human-driver (lower lateral jerk and lower smoothness $^{-1}$ ). The motion curvature  $\kappa(t)$  of one lane change sample for computer motion generated and human-driver is shown in Fig. 18. As shown in this sample, the computer generated smoother motion (lower curvature) compared to human-driver.

## V. Conclusions

In this paper, a behavior/motion model for automated lane change at expressway has been proposed. The proposed model is mainly inspired by human-driver lane change and behavior data that can handle difficult lane change scenarios. The occupancy grid states are categorized and alternative behaviors are defined for each corresponding category. To select the suitable behavior,  $dx/dv$  graph is segmented based on the human-driver lane change patterns. Our experiments were carried on at the expressway where the lanes have different ranges of velocity. In this case, change to left or right lane means change to slower or higher speed lane. Thus, the segmented  $dx/dv$  will be dependent on the left or right lane change. The proposed model is intuitive and able to handle

complicated lane change scenarios even in the presence of disturbances or sudden changes in behavior of surrounding vehicles. In future research, more human-driver lane change patterns are going to be extracted for better segmentation of  $dx/dv$  graph, and also more comparison with related works will be added. Our current behavior model does not consider the interaction between the vehicles so that in future work, our model will consider it.

## About the Authors



**Quoc Huy Do** received his B.S. and M.S. degrees in Information Technology from Hanoi University of Technology, Vietnam, in 2006 and 2008, respectively. He served on the faculty of Hanoi University of Science and Technology in the academic years of 2006–2009. He received his Ph.D. in information and systems from Toyota Technological Institute (TTI) in 2013. Currently, he is a post-doctoral fellow at Research Center for Smart Vehicles of TTI. His research field is path planning, vehicle dynamic and automated lane change for autonomous vehicles.



**Seiichi Mita** received his B.S., M.S., and Ph.D. degrees in electrical engineering from Kyoto University in 1969, 1971, and 1989, respectively. He studied at Hitachi Central Research Laboratory, Kokubunji, Japan, from 1971 to 1991, investigating signal processing and coding methods. Currently, he is a professor at Toyota Technological Institute (TTI) in Nagoya (since 1999) and a director of the Research Center for Smart Vehicles at TTI. Currently, he is greatly interested in the research area of autonomous vehicles and sensing systems. Dr. Mita is a member of IEEE. He received the best paper award from the IEEE Consumer Electronics Society in 1986.



**Hossein Tehrani Nik Nejad** received his B.S. and M.S. degrees in industrial engineering from Sharif University of Technology, Iran, in 1996 and 1998, respectively. He received his Ph.D. degree in mechanical engineering from Osaka Prefecture University, Japan, in 2009. In 2009, he joined the Toyota Technological Institute at Japan as Post-doctoral Fellow in the Smart Vehicle Center. In 2012, he joined the DENSO CORPORATION. Dr. Tehrani is an IEEE member and also a technical committee member of ITS-Nagoya chapter. His research interests are automated driving, sensor processing, machine learning and deep neural networks.



**Masumi Egawa** received his the B.E. and M.S. degrees from Nagoya Institute of Technology, in Nagoya, Japan, in 1996 and 1998 respectively. He currently works for DENSO CORPORATION.

His research interests have been in information security, wireless communication, and applications of machine learning methods.



**Kenji Muto** received the M.S. degree in Electronic-Mechanical Engineering from Nagoya University in 1997. He currently works for research and development department in DENSO CORPORATION. His research interests have been in vehicular sensing and communication system and its applications.



**Keisuke Yoneda** received his B.S. degrees in engineering from Toyohashi University of Technology in 2007, and M.S., and Ph.D. degrees in information science from Hokkaido University in 2009 and 2012, respectively. He is currently work as Assistant Professor at Autonomous Vehicle Research Unit of Institute for Frontier Science Initiative, Kanazawa University. He is interested in the research area of autonomous vehicles, artificial intelligence and artificial life. He is a member of the Japan Society for Precision Engineering and the Society of Automotive Engineers of Japan, Inc.

## References

- [1] Volvo Trucks. (2015). European accident research and safety report [Online]. Available: [http://www.volvotrucks.com/SiteCollectionDocuments/VTC/Corporate/Values/ART%20Report%202015\\_150dpi.pdf](http://www.volvotrucks.com/SiteCollectionDocuments/VTC/Corporate/Values/ART%20Report%202015_150dpi.pdf)
- [2] L. Fletcher, et al., "The DARPA urban challenge," in *Springer Tracts in Advanced Robotics*, vol. 56. Berlin: Springer, 2009, pp. 509–548.
- [3] W. He, X. Wang, G. Chen, M. Guo, T. Zhang, P. Han, and R. Zhang, "Monocular based lane-change on scaled-down autonomous vehicles," in *Proc. IEEE Intelligent Vehicles Symp.*, 2011, pp. 144–149.
- [4] W. Dolan and B. Litkouhi, "A prediction- and cost function-based algorithm for robust autonomous freeway driving," in *Proc. IEEE Intelligent Vehicles Symp.*, 2010, pp. 512–517.
- [5] D. Kasper, G. Weidl, and T. Dang, et al., "Object-oriented Bayesian networks for detection of lane change maneuvers," *IEEE Intell. Transp. Syst. Mag.*, vol. 4, no. 1, pp. 19–31, 2014.
- [6] D. Kasper, G. Weidl, and T. Dang, et al., "Object-oriented Bayesian networks for detection of lane change maneuvers," in *Proc. IEEE Intelligent Vehicles Symp.*, 2010, pp. 673–678.
- [7] R. Schubert, K. Schulze, and G. Wanielik, "Situation assessment for automated lane-change maneuvers," *IEEE Trans. Intell. Transp. Syst.*, vol. 11, no. 3, pp. 607–616, 2010.
- [8] S. Sivaraman and M. M. Trivedi, "Dynamic probabilistic drivability maps for lane change and merge driver assistance," *IEEE Trans. Intell. Transp. Syst.*, vol. 15, pp. 2063–2073, 2014.
- [9] R.S. Tomar, S. Verma, and G.S. Tomar, "Prediction of lane change trajectories through neural network," in *Proc. Int. Conf. Computational Intelligence and Communication Networks*, 2010, pp. 249–255.
- [10] A. Polychronopoulos, M. Tsogas, and A. Amiditis, et al., "Dynamic situation and threat assessment for collision warning systems: the euclidean approach," in *Proc. IEEE Intelligent Vehicles Symp.*, 2004, pp. 636–641.
- [11] T. Gindel, S. Brechtel, and R. Dillmann, "A probabilistic model for estimating driver behaviors and vehicle trajectories in traffic environments," in *Proc. Int. IEEE Conf. Intelligent Transportation Systems*, 2010, pp. 1625–1631.
- [12] J. Schlechtriemen, A. Wedel, J. Hillenbrand, G. Breuel, and K. Kuhnert, "A lane change detection approach using feature ranking with maximized predictive power," in *Proc. IEEE Intelligent Vehicles Symp.*, 2014, pp. 108–114.
- [13] J. Schlechtriemen, F. Wirthmueller, A. Wedel, G. Breuel, and K. D. Kuhnert, "When will it change the lane? A probabilistic regression approach for rarely occurring events," in *Proc. IEEE Intelligent Vehicles Symp.*, 2015, pp. 1573–1579.
- [14] P. Kumar, M. Perrollaz, S. Lefevre, and C. Laugier, "Learning-based approach for online lane change intention prediction," in *Proc. IEEE Intelligent Vehicles Symp.*, 2015, pp. 797–802.
- [15] E. Naranjo, C. Gonzalez, R. Garcia, and T. de Pedro, "Lane-change fuzzy control in autonomous vehicles for the overtaking maneuver," *IEEE Trans. Intell. Transp. Syst.*, vol. 9, no. 5, pp. 458–450, 2008.
- [16] M. Bahrami, A. Wolf, M. Aeberhard, and D. Wollherr, "A prediction-based reactive driving strategy for highly automated driving function on freeways," in *Proc. IEEE Intelligent Vehicles Symp.*, 2014, pp. 400–406.
- [17] J. Nilsson and J. Sjöberg, "Strategic decision making for automated driving on two-lane, one way roads using model predictive control," in *Proc. IEEE Intelligent Vehicles Symp.*, 2015, pp. 1253–1258.
- [18] Y. Du, Y. Wang, and C. Chan, "Autonomous lane-change controller via mixed logical dynamical," in *Proc. 17th Int. Conf. Intelligent Transportation Systems*, 2014, pp. 1154–1159.
- [19] Y. Du, Y. Wang, and C. Chan, "Autonomous lane-change controller," in *Proc. IEEE Intelligent Vehicles Symp.*, 2015, pp. 386–393.
- [20] U. Simon and M. Markus, "Probabilistic online POMDP decision making for lane changes in fully automated driving," in *Proc. IEEE Conf. Intelligent Transportation Systems*, 2015, pp. 2063–2070.
- [21] S. Brechtel, T. Gindel, and R. Dillmann, "Probabilistic MDP-behavior planning for cars," in *Proc. 14th Int. IEEE Conf. Intelligent Transportation Systems*, 2011, pp. 1537–1542.
- [22] M. Ardel, C. Coester, and N. Kaempchen, "Highly automated driving on freeways in real traffic using a probabilistic framework," *IEEE Trans. Intell. Transp. Syst.*, vol. 13, no. 4, pp. 1576–1585, 2012.
- [23] Q. Jin, G. Wu, K. Boriboonsomsin, and M. Barth, "Improving traffic operations using real-time optimal lane selection with connected vehicle technology," in *Proc. IEEE Intelligent Vehicles Symp.*, 2014, pp. 70–75.
- [24] H. Jula, E. Kosmatopoulos, and P. Ioannou, "Collision avoidance analysis for lane changing and merging," *IEEE Trans. Veh. Technol.*, vol. 49, pp. 2295–2308, 2000.
- [25] C. Rodemerck, S. Habenicht, A. Weitzel, H. Winner, and T. Schmitt, "Development of a general criticality criterion for the risk estimation of driving situations and its application to a maneuver-based lane change assistance system," in *Proc. IEEE Intelligent Vehicles Symp.*, 2012, pp. 264–269.
- [26] G. Schildbach and F. Borrelli, "Scenario model predictive control for lane change assistance on highways," in *Proc. IEEE Intelligent Vehicles Symp.*, 2015, pp. 611–616.
- [27] J. Ziegler, P. Bender, T. Dang, and C. Stiller, "Motion planning for Bertha: a local, continuous method," in *Proc. Intelligent Vehicles Symp.*, Dearborn, MI, 2014, pp. 450–457.
- [28] Q. H. Do, L. Han, H. Tehrani, and S. Mita, "Safe path planning among multi obstacles," in *Proc. IEEE Intelligent Vehicles Symp.*, 2011, pp. 552–558.
- [29] H. Tehrani, K. Muto, K. Yoneda, and S. Mita, "Evaluating human & computer for expressway lane changing," in *Proc. IEEE Intelligent Vehicles Symp.*, 2014, pp. 382–387.
- [30] Q. H. Do, H. Tehrani, M. Egawa, K. Muto, K. Yoneda, and S. Mita, "Distance constraint model for automated lane change to merge or exit," in *Proc. 3rd Int. Symp. Future Active Safety Technology Towards Zero Traffic Accidents*, 2015, pp. 17–24.
- [31] H. Tehrani, Q. H. Do, M. Egawa, K. Muto, K. Yoneda, and S. Mita, "General behavior and motion model for automated lane change," in *Proc. IEEE Intelligent Vehicles Symp.*, 2015, pp. 1154–1159.
- [32] "Merging and passing," in *California Driver Handbook—Safe Driving Practices*. Sacramento, CA: California Department of Motor Vehicles, 2012.
- [33] M. Werling, J. Zeigler, S. Kammerl, and S. Thrun, "Optimal trajectory generation for dynamic street scenarios in a Frenet frame," in *Proc. IEEE Int. Conf. Robotic and Automation*, 2010, pp. 987–995.
- [34] D. Althoff, M. Buss, A. Lawitzky, M. Werling, and D. Wollherr, "On-line trajectory generation for safe and optimal vehicle motion planning," *AMS*, pp. 99–107, 2012.
- [35] T. Fraichard and H. Asama, "Inevitable collision states. A step towards safer robots?," *Adv. Robotics*, vol. 18, pp. 1001–1024, 2004.
- [36] L. Peng, A. Kurt, and U. Özgüner, "Trajectory prediction of lane changing vehicle based on driver behavior estimation and classification," in *Proc. Intelligent Transportation Systems*, 2014, pp. 942–947.
- [37] Y. Kanayama and G. R. D. Haan, "Least cost paths with algebraic cost functions," in *Proc. IEEE Int. Workshop Intelligent Robots*, 1988, pp. 541–546.